

THE MINIMUM UNIVERSAL METAL DENSITY BETWEEN REDSHIFTS 1.5 AND 5.5

ANTOINETTE SONGAILA¹

Institute for Astronomy, University of Hawaii, 2680 Woodlawn Drive, Honolulu, HI 96822

Accepted for publication in Astrophysical Journal Letters

ABSTRACT

It appears that the Lyman α forest is becoming thick at a redshift of about 5.5, cutting off the higher redshift intergalactic medium from view in neutral hydrogen. However, the effects of star formation at higher redshift are still readable in the intergalactic metal lines. In this paper I use observations of 32 quasars with emission redshifts in the range 2.31 to 5.86 to study the evolution of the intergalactic metal density from $z = 1.5$ to $z = 5.5$. The C IV column density distribution function is consistent with being invariant throughout this redshift range. From direct integration, I determine Ω_{CIV} to be in the range $(2.5 - 7) \times 10^{-8}$ and Ω_{SiIV} in the range $(0.9 - 3) \times 10^{-8}$ between $z = 1.5$ and $z = 5$. The metallicity at $z = 5$ exceeds 3.5×10^{-4} , which in turn implies that this fraction of the universal massive star formation took place beyond this redshift. This is sufficient to have ionized the intergalactic medium.

Subject headings: early universe — intergalactic medium — quasars: absorption lines — galaxies: formation

1. INTRODUCTION

The epoch of reionization is the ultimate depth to which we can directly investigate neutral hydrogen in the intergalactic medium (IGM). Whether or not it signals the onset of reionization, the increasing optical depth of the Lyman α forest at redshifts above 5 (Becker et al. 2001; Djorgowski et al. 2001; Fan et al. 2000b, 2001c; Songaila et al. 1999) severely limits our ability to study the IGM with neutral hydrogen at these times. However, we can continue to study the metal lines in the quasar spectra, and in particular the C IV ‘forest’. These absorption lines can be used to infer the history of early star formation by mapping the evolution of the universal density of metals with redshift. The contribution to the universal metallicity arising from the diffuse IGM has been extensively analyzed at redshift $z \sim 3$ (Cowie et al. 1995, Tytler et al. 1995, Songaila 1997, Songaila 1998, Ellison et al. 2000) and some information is also available from investigations of O VI at lower redshift (Burles & Tytler 1996, Tripp, Savage & Jenkins 2000). However, to date there has been no systematic analysis of the variation of the intergalactic metal density as a function of redshift.

Most interpretations of the origin of the $z = 3$ metallicity have focussed on ejection or stripping of material from small galaxies that formed at higher redshifts ($z > 5$) (Gnedin & Ostriker 1997, ; Gnedin 1998; Madau, Ferrara & Rees 2001). It is also possible that the metals may originate in genuine Population III star formation at very high redshift (e.g., Carr, Bond & Arnett 1984; Ostriker & Gnedin 1996; Haiman & Loeb 1997; Abel et al. 1998). In these scenarios most of the IGM metals would be in place at the highest currently observable redshifts. More recently, Steidel has suggested that the observed metals may instead originate in extremely fast winds from Lyman break galaxies at $z = 3$ (e.g. Pettini 2001). Such a model may already encounter problems in explaining the kinematic quiescence of the C IV lines (Rauch, Sargent & Barlow 2001) but it can also be tested by determining

whether the metallicity changes with redshift.

This paper analyses the distribution of C IV and Si IV ions in the IGM over a wide range of redshifts from $z = 1.5$ to $z = 5.5$ using newly-discovered Sloan Digital Sky Survey (SDSS) quasars (Anderson et al. 2001; Fan et al. 1999, 2000a,b, 2001a,b; Zheng et al. 2000) to provide a high redshift sample. I use the methodology previously applied at $z \sim 3$ (Songaila 1997) of directly integrating the observed ion column densities in Ly α forest clouds to obtain strict lower limits on Ω_{ion} , which, with plausible assumptions on ionization corrections and abundance patterns, can provide a strict lower limit on Ω_{metals} at a number of redshifts.

New observations of $z = 2 - 3$ quasars with the HIRES spectrograph (Vogt 1994) on the KeckI telescope and of $z = 4 - 5.8$ quasars with the ESI instrument (Sheinis et al. 2000) on KeckII are described in section 2. In section 3 I construct column density distribution functions for C IV and Si IV from $z = 1.5$ to $z = 5.5$ and perform the integrations. Conclusions are given in section 4.

2. OBSERVATIONS

The data used in the paper comprise HIRES observations of 13 quasars reported in Songaila (1998) together with HIRES and ESI observations of a further 19 quasars. The reduction of the HIRES (lower redshift) observations follows the procedures given in Songaila (1998). The fainter, high redshift, quasars were observed with the ESI instrument in echelle mode. (See Songaila (2001) for a list of quasars observed with ESI.) The resolution in this configuration is comparatively low, ~ 5300 for the 0.75" slit width used, but the red sensitivity is high and the wavelength coverage is complete from 4000 Å to 10,000 Å. At the red wavelengths, precision sky subtraction is required since the sky lines can be more than two orders of magnitude brighter than the quasars. In order to deal with this issue, individual half-hour exposures were made, stepped along the slit, and the median was used to pro-

¹Visiting astronomer, W. M. Keck Observatory, jointly operated by the California Institute of Technology and the University of California.

vide the primary sky subtraction. The frames were then registered, filtered to remove cosmic rays and artifacts, and then added. At this point a second linear fit to the slit profile in the vicinity of the quasar was used to remove any small residual sky. The observations were made at the parallactic angle and flux calibrated using observations of white dwarf standards scattered through the night. These standards were also used to remove telluric absorption features in the spectra, including the various atmospheric bands. The final extractions of the spectra were made using a weighting provided by the profile of the white dwarf standards. Wavelength calibrations were obtained using third-order fits to CuAr and Xe lamp observations at the beginning and end of each night, and the absolute wavelength scale was then obtained by registering these wavelength solutions to the night sky lines. The wavelengths and redshifts are given in the vacuum heliocentric frame.

I next constructed the sample of all C IV and Si IV absorption lines which lie more than 50 Å longward of each quasar's Lyman alpha emission and hence clearly outside the Lyman alpha forest region. The doublets were found by inspection of the spectra, and confirmed by consistency of the column density and velocity structure in the two members of the doublet. Systems within 5000 km s⁻¹ of the quasar's emission redshift were excluded to avoid contaminating the sample with proximate systems whose ionization may be dominated by the quasar itself. The final C IV sample consists of 367 C IV doublets, with $1.74 \leq z \leq 5.29$ and $12.0 \leq \log(N_{\text{C IV}}) \leq 14.9$. The Si IV sample contains 109 systems between $z = 1.78$ and $z = 5.29$, with $12.0 \leq \log(N_{\text{Si IV}}) \leq 14.8$.

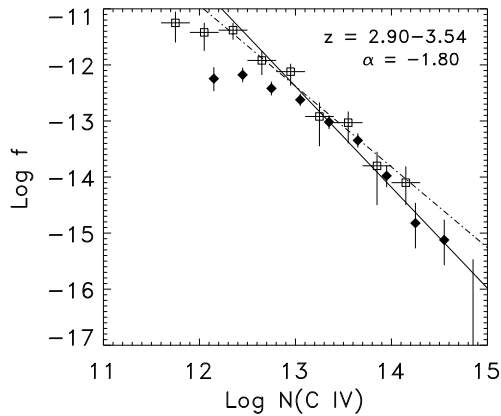


FIG. 1.— Column density distribution of C IV absorbers for the present sample (filled symbols) in the redshift interval $2.90 < z < 3.54$; f is the number of systems per column density interval per unit redshift path. The bin size is $10^{0.3} N \text{ cm}^{-2}$ and the error bars are $\pm 1\sigma$ based on the number of points in each bin. The solid line is a power law of the form $f(N)dN = BN^{-\alpha}dN$ with index $\alpha = 1.8 \pm 0.1$ established by a maximum likelihood fit to all systems with $N(\text{CIV}) \geq 10^{13} \text{ cm}^{-2}$. The open symbols are the column density distribution of Ellison et al. (2000) for C IV absorbers in the quasar Q1422+231 over the same redshift interval (not corrected for incompleteness at low N). The dot-dash line is Ellison et al.'s power law fit with index 1.44 ± 0.05 to $N(\text{CIV}) = 10^{12} \text{ cm}^{-2}$.

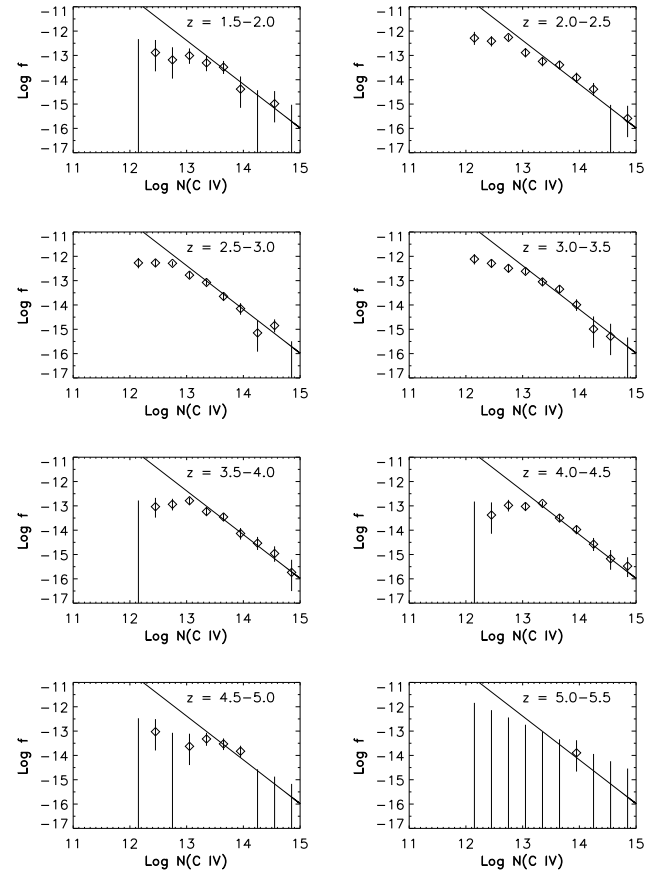


FIG. 2.— Column density distribution of C IV absorbers as in Figure 1 for various redshift ranges. In each redshift interval, the solid line is the fiducial power law $f(N)dN = BN^{-\alpha}dN$ with the normalization and index $\alpha = 1.8$ established from Figure 1.

In all cases, ion column densities were determined by fitting up to ten Voigt profiles to each redshift system, defined to be all absorption near a given fiducial redshift with gaps in velocity space of no more than 50 km s⁻¹. The column density at a given redshift is then the total column density of all such components. In all but a few systems, individual lines were unsaturated, so that fitted column densities are insensitive to b -value. For the ESI spectra, where the lower resolution observations make this issue more critical, I adopted in doubtful cases a column density based on assuming that the weaker member of the doublet was unsaturated. This provides a minimum estimate of the column density.

3. DISTRIBUTION FUNCTIONS

With these samples, the column density distribution function $f(N)$ was determined for each ion. $f(N)$ is defined as the number of absorbing systems per unit redshift path per unit column density, where at a given redshift z the redshift path, $X(z)$ is defined as $X(z) \equiv \frac{2}{3}[(1+z)^{3/2} - 1]$ for $q_0 = 0.5$ (Tytler 1987). Throughout the paper the distributions are calculated in c.g.s. units and are plotted with 1σ error bars calculated from the Poisson errors based on the number of systems in each bin (Gehrels 1986). In addition, all calculations were made assuming a $q_0 = 0.5$, $\Lambda = 0$ cosmology, which is a good approximation to the currently favored Λ -dominated cos-

mologies above about $z = 1$.

In Figure 1 I show the column density distribution in the redshift interval $2.90 < z < 3.54$ and compare this with the distribution over the same redshift range from an extremely deep exposure of the quasar 1422+231, as reported in Ellison et al. (2000). From the figure it can be seen that the present data become incomplete below a column density of approximately 10^{13} cm^{-2} in this redshift range. Above this value a maximum likelihood fit to a power law slope gives an index of $\alpha = 1.8 \pm 0.1$. This is steeper than the Ellison et al. fit of 1.44 ± 0.05 based on the more limited sample, but in fact provides a good fit to those data points at column densities less than 10^{13} cm^{-2} and to the corrected counts in 1422+231 at less than 10^{12} cm^{-2} . I adopt this fit, with a normalization of $\log f = -12.4$ at a column density of 10^{13} cm^{-2} , as a fiducial to compare with the distributions in other redshift ranges.

The C IV and Si IV distribution functions are shown as a function of redshift in Figure 2. For redshifts less than 4 the data is drawn from HIRES observations of relatively bright quasars, and significant incompleteness occurs only below column densities of about 10^{13} cm^{-2} . At higher redshifts, where most of the observations are from ESI and the quasars are fainter, simulations show there is clearly incompleteness even above this column density. In the highest redshift bin, 5–5.5, lying at the longest wavelengths where the night sky is highest, recovery of lines is quite sporadic and the sample is extremely incomplete. Over the column density range in which incompleteness is not a problem, the distributions are consistent with being invariant throughout the range of redshifts sampled.

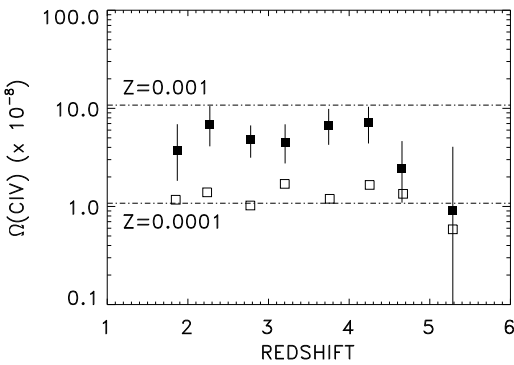


FIG. 3.— $\Omega(\text{CIV})$ as a function of redshift plotted from the data of Table 1 ($H_0 = 65 \text{ km s}^{-1} \text{ Mpc}^{-1}$ and $q_0 = 0.5$). In each redshift interval, the filled symbols show $\Omega(\text{CIV})$ computed for all systems with $10^{12} \text{ cm}^{-2} \leq N(\text{CIV}) \leq 10^{15} \text{ cm}^{-2}$, whereas the open symbols are $\Omega(\text{CIV})$ computed for all systems with $10^{13} \text{ cm}^{-2} \leq N(\text{CIV}) \leq 10^{14} \text{ cm}^{-2}$. Symbols are plotted at the average redshift for each bin (Table 1). Error bars are 90% confidence limits computed using Monte Carlo simulations. The dot-dash lines are $\Omega(\text{CIV})$ computed assuming $\Omega_b h^2 = 0.023$, $h = 0.65$, a C IV ionization fraction of 0.5 and metallicities $Z = 0.0001$ and 0.001, respectively.

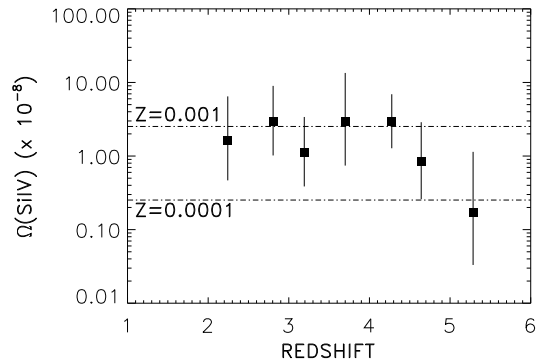


FIG. 4.— As in Fig. 3, for Si IV.

$\Omega_{\text{C IV}}$ and $\Omega_{\text{Si IV}}$ were next calculated from the line samples in each redshifts interval according to

$$\Omega_{\text{ion}} = \frac{H_0}{c \rho_{\text{crit}}} (1 + 2q_0 z)^{\frac{1}{2}} \frac{\sum N_{\text{ion}}}{\Delta X} m_{\text{ion}} \quad (1)$$

where $\rho_{\text{crit}} = 1.89 \times 10^{-29} h^2 \text{ g cm}^{-3}$ is the cosmological closure density, m_{ion} is the ion's mass, and $H_0 = 100h \text{ km s}^{-1} \text{ Mpc}^{-1}$. The values of $\Omega_{\text{C IV}}$ and $\Omega_{\text{Si IV}}$ are plotted in Figures 3 and 4 and tabulated in Table 1 for $H_0 = 65 \text{ km s}^{-1} \text{ Mpc}^{-1}$ and $q_0 = 0.5$ (Ω_{ion} scales as $h^{-1} [1 + 2q_0 z]^{1/2}$.) The error bars are 90% confidence limits; they were computed by using the power-law distribution with the shape of the fiducial fit, and normalized to match the measured Ω_{ion} , to generate Monte Carlo simulations of line lists and then measuring Ω_{ion} from these simulations.

4. DISCUSSION

If the ionization fraction can be estimated, then Ω_{ion} can be translated to Ω_{element} for each element in question. I shall assume here that C IV and Si IV are the dominant ionization stages with ionization fractions of 0.5 (Songaila 1997). This assumption is conservative in that it will, if anything, underestimate the resulting metallicity since neither C IV nor Si IV can be a much larger fraction than this; even in the extreme case, the metallicity will be overestimated by no more than a factor of two. The measurements of Ω_{element} can then be compared with measurements of Ω_b to obtain the universal metallicity contribution of the gas. (The inverse procedure of guessing a metallicity and then using this to estimate Ω_b has been followed by Tripp, Savage & Jenkins (2000) in analyzing O VI measurements at low redshift. However, given that we know Ω_b from other sources, it seems more reasonable in the present case to use that value to constrain the metallicity.) A value of $\Omega_b h^2 = 0.023 \pm 0.003$ is adopted from measurements of the microwave background (Netterfield et al. 2001), which is consistent with the most recent deuterium estimates (e.g., Tytler et al. 2001). The metallicity is quoted relative to solar values of 3.3×10^{-4} for carbon and 3.3×10^{-5} for silicon (Anders & Grevesse 1989). The results of this procedure are illustrated with the dashed lines in Figures 3

and 4. For $h = 0.65$, I conclude that the carbon metallicity is 5×10^{-4} at lower redshifts and still exceeds 2×10^{-4} at $z = 5$. The silicon metallicity is about 2 times higher, 3.5×10^{-4} at $z = 5$, with the assumed Si IV ionization fraction of 0.5. This presumably reflects the faster generation of the alpha process elements, but the exact amount of the excess of silicon over carbon will of course depend on the relative Si IV and C IV ionization fractions.

The minimum nature of the estimates should be emphasized: in any given region, only observed metals are counted. While we believe that the bulk of the baryons are to be found in these clouds at these redshifts (Rauch et al. 1997; Kim et al. 1997), the bulk of the metals may not, and may instead be primarily retained in the galaxies that generated them. Furthermore, the assumption that C IV and Si IV are dominant ionization stages depends critically on the shape and intensity of the metagalactic ionizing radiation field and on the densities of the clouds. There may be cloud column densities and epochs for which this assumption is no longer true and where the observed ion densities would imply higher metallicities. Finally, the high noise levels at the longest wavelengths mean we are substantially undercounting the lines at the highest redshifts, and the turndown in the ion densities at these redshifts may be due to this effect rather than to a real physical change. Simulations of the incompleteness above $z = 4.5$ suggest that C IV line identification is substantially complete to $\log N = 13.25$ at $z = 4.5$ and to $\log N = 13.7$ above $z = 5$, resulting in corrections to $\Omega(\text{C IV})$ of factors of 1.35 and 1.67, respectively, in these two bins.

Despite these caveats we can still draw some substantial conclusions. First, since total metal densities are dominated by oxygen, which we expect to scale most closely with silicon, we would conclude that a minimum universal metallicity of about 3.5×10^{-4} of the solar metallicity is in place at $z = 5$. This means that this fraction of the universal massive star formation should have taken place before this time, and this in turn can be translated to a number of ionizing photons per baryon. Since a metallicity of 10^{-5} gives rise to one ionizing photon per baryon (e.g., Miralda-Escudé & Rees 1997), the metallicity measured at $z = 5$ is sufficient to have preionized the IGM.

Second, there appears to have been little change in the universal ion densities since $z = 5$. It is possible that this could be caused by matched variations in the ionization parameter and the metallicity. However, at least above $z \sim 3$, where the metagalactic ionizing spectrum is likely to be galaxy-dominated (e.g. Steidel et al. 2001), C IV and Si IV will be the dominant ionization stages, and it appears more likely that the metal densities have remained relatively constant during this period. Although this does not rule out the possibility of additional contributions from mechanisms such as galactic winds, it does suggest that, to a large extent, the metals observed in the intergalactic medium at $z = 3$ have an earlier origin.

This research was supported by the National Science Foundation under grants AST 96-17216 and AST 00-98480.

REFERENCES

Abel, T., Anninos, P., Norman, M. L. & Zhang, Y. 1998, ApJ, 508, 518.
 Anders, E., & Grevesse, N. 1989, Geochim. Cosmochim. Acta, 53, 197.
 Anderson, S. F., et al. 2001, AJ, 122, 503.
 Becker, R. H., et al. 2001, preprint (astro-ph/0108097).
 Burles, S. & Tytler, D. 1996, 460, 584.
 Carr, B. J., Bond, J. R. & Arnett, W. D. 1984, ApJ, 277, 445.
 Cowie, L. L., Songaila, A., Kim, T.-S., & Hu, E. M. 1995, AJ, 109, 1522.
 Djorgovski, S. G., Castro, S. M., Stern, D. & Mahabel, A. A. 2001, preprint (astro-ph/0108069).
 Ellison, S. L., Songaila, A., Schaye, J. & Pettini, M. 2000, AJ, 120, 1175.
 Fan, X., et al. 1999, AJ, 118, 1.
 Fan, X., et al. 2000a, AJ, 119, 1.
 Fan, X., et al. 2000b, AJ, 120, 1167.
 Fan, X., et al. 2001a, AJ, 121, 31.
 Fan, X., et al. 2001b, AJ, 121, 54.
 Fan, X. et al. 2001c, preprint (astro-ph/0108063).
 Gehrels, N. 1986, ApJ, 303, 336.
 Gnedin, N. Y., & Ostriker, J. P. 1997, ApJ, 486, 581.
 Gnedin, N. Y. 1998, MNRAS, 294, 407.
 Haiman, Z. & Loeb, A. 1997, ApJ, 483, 21.
 Kim, T.-S., Hu, E. M., Cowie, L. L. & Songaila, A. 1997, AJ, 114, 1.
 Madau, P., Ferrara, A. & Rees, M. J. 2001, ApJ, 555, 92.
 Miralda-Escudé, J. & Rees, M. J. 1997, ApJ 478, L57.
 Netterfield, C. B., et al. 2001, preprint (astro-ph/0104460).
 Ostriker, J. P. & Gnedin, N. Y. 1996, ApJ, 472, L63.
 Pettini, M. 2001, in Chemical Enrichment of the Intracluster and Intergalactic Medium, ed. F. Matteucci, (San Francisco: ASP), in press.
 Rauch, M., Haehnelt, M. G. & Steinmetz, M. 1997, ApJ, 481, 601.
 Rauch, M., Sargent, W. L. W. & Barlow, T. A. 2001, ApJ, 554, 823.
 Sheinis, A. I., Miller, J. S., Bolte, M. & Sutin, B. M. 2000, Proc. SPIE, 4008, 522.
 Songaila, A. 1997, ApJ, 490, L1.
 Songaila, A. 1998, AJ, 115, 2184.
 Songaila, A., Hu, E. M., Cowie, L. L. & McMahon, R. G. 1999, ApJ, 525, L5.
 Songaila, A. 2001, in preparation.
 Steidel, C. C., Pettini, M. & Adelberger, K. L. 2001, ApJ, 546, 665.
 Tripp, T. M., Savage, B. D. & Jenkins, E. B. 2000, ApJ, 534, L1.
 Tytler, D., Fan, X.-M., Burles, S., Cottrell, L., Davis, C., Kirkman, D., & Zuo, L. 1995, in QSO Absorption Lines, ed. G. Meylan (Heidelberg: Springer), 289.
 Tytler, D. 1987, ApJ, 321, 49.
 Tytler, D., O'Meara, J. M., Suzuki, N. & Lubin, D. 2001, Phys. Scr., in press.
 Vogt, S. S. et al. 1994, Proc. SPIE, 2198, 362.
 Zheng, W., et al. 2000, AJ, 120, 1607.

TABLE 1
 Ω_{CIV} AND Ω_{SiIV} BY REDSHIFT

z	ΔX C IV	$\langle z \rangle$ C IV	# Lines C IV	Ω_{CIV} ($\times 10^{-8}$)	ΔX Si IV	$\langle z \rangle$ Si IV	# Lines Si IV	Ω_{SiIV} ($\times 10^{-8}$)
1.5 – 2.0	3.54	1.869	14	3.74				
2.0 – 2.5	7.22	2.272	59	6.83	3.67	2.243	13	1.65
2.5 – 3.0	11.08	2.779	88	4.79	6.05	2.806	15	2.90
3.0 – 3.5	7.46	3.206	67	4.50	5.58	3.192	28	1.13
3.5 – 4.0	10.49	3.746	55	6.71	2.66	3.700	8	2.91
4.0 – 4.5	11.93	4.240	67	7.18	9.69	4.277	31	2.97
4.5 – 5.0	5.36	4.655	16	2.46	4.35	4.642	9	0.85
5.0 – 5.5	1.25	5.285	1	0.90	1.25	5.285	1	0.17